Comparison of Wave Sensing Stragegies for Active Structural Acoustic Control

P. Audrain, P. Masson and A. Berry
G.A.U.S., Université de Sherbrooke, Sherbrooke, Québec, J1K2R1, Canada

1 Introduction

Among the strategies available for the active control of energy transmission from one area of a structure to another area, the control of travelling waves, structural intensity or power flow can all be considered. The previous intensity or power flow control strategies usually assumed far field propagation and are based on an estimate of the exact structural energy flow [1, 2].

It is thererefore the purpose of this paper to present a strategy using strain sensing for the control of structural intensity associated with flexural motion in a coupled beam/plate mechanical system and compare it with a strategy based on the control of the acceleration at one point on the structure. The instantaneous intensity is completely taken into account in the control algorithm, *i.e.* all the terms are considered in the real-time control process and, in particular, the evanescent waves are considered in this approach. Previous work has shown the validity of this energy-based approach using acceleration sensing [3]. The approach is limited to cases where the geometry is such that the intensity at the error sensor will have the same sign for the control source and the primary disturbance.

2 Structural intensity measurement using strain sensing

2.1 Flexural structural intensity in a beam

The structural intensity is the instantaneous rate of vibrational energy transfer, or energy flow, per unit area in a given direction. The instantaneous energy flow in a beam, called the instantaneous structural intensity (subscript $_i$) in this paper, originating from a flexural displacement $w(x,t)$, can be expressed for an Euler-Bernoulli isotropic beam:

$$\vec{I}_i^f = \left(EI\frac{\partial^3 w}{\partial x^3}\right)\left(\frac{\partial w}{\partial t}\right)\vec{i} - \left(EI\frac{\partial^2 w}{\partial x^2}\right)\left(\frac{\partial^2 w}{\partial t \partial x}\right)\vec{i} \quad (1)$$

where E is the Young's modulus, I the area moment of inertia of the beam and $\vec{i}$ the unit vector in the x direction. The control algorithm will minimize the time average of the instantaneous intensity, called the active intensity.

2.2 Finite differences implementation

Since four discrete strain sensors are used to estimate the structural intensity, it is necessary to develop a finite differences approximation based on strain sensing to measure structural intensity associated with flexural motion in beams. The flexural strain ε_z is related to the flexural displacement by $\varepsilon_z(x,t) = \dfrac{\partial^2 w(x,t)}{\partial x^2}$. The instantaneous intensity is evaluated at the center of the probe, x_e, with an error on the order of Δ, Δ being the spacing between two consecutive sensors. The time differentials of strain in equation (1) are estimated using a backward finite difference scheme with error on the order of τ^2, where τ is the time increment between samples.

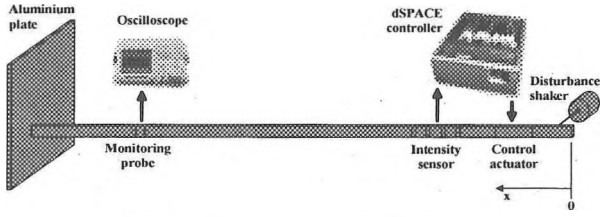

Figure 1: Experimental setup.

3 Experimental validation

3.1 Experimental setup

The Fig. 1 shows the experimental setup used for the control. The structure is a plate ($0.48m \times 0.42m \times 0.003m$) connected to a beam ($3m \times 0.0254m \times 0.003m$) made of aluminium covered on one side by a *ISD 830* viscoelastic material combined with a constraining aluminium foil. The viscoelastic material is used to increase the structural damping such that the intensity signal can be measured.

The disturbance is generated by a *Bruel & Kjaer 4810* shaker connected to the beam by a stinger at one end of the beam. The control actuator consists of a PZT patch actuator (*PSI-5A-S2*). The coordinates of the edges of the patch are $0.2m$ and $0.27m$ from the shaker taken as the origin of coordinates. The coordinates of the four PVDF strain sensors are $x_1 = 0.22m$, $x_2 = 0.26m$, $x_3 = 0.3m$ and $x_4 = 0.34m$. The accelerometer used for acceleration control is located in the middle of the PVDF sensors array at $x_e = 26.5cm$. Two accelerometers located at $2.09m$ and $2.19m$ are used for monitoring the control and the mean RMS value of these signals is used as a performance indicator.

$$\overline{\boldsymbol{H}}(s,\beta) = -\hat{\boldsymbol{h}}(s)\,\boldsymbol{C}(s,\beta)\,\left[\boldsymbol{I} - \hat{\boldsymbol{h}}(s)\,\boldsymbol{C}(s,\beta)\right]^{-1} \quad (5)$$

$$\boldsymbol{L}_{\boldsymbol{H}}(s) = [\,\boldsymbol{h}(s) - \hat{\boldsymbol{h}}(s)\,]\,\hat{\boldsymbol{h}}^{-1}(s) \quad (6)$$

$$\boldsymbol{C}(s,\beta) = [\boldsymbol{I} + \boldsymbol{\Gamma}(\beta)\,\hat{\boldsymbol{h}}(s)]^{-1}\,\boldsymbol{\Gamma}(\beta) \quad (7)$$

$$\boldsymbol{\Gamma}(\beta) = diag\left\{\frac{-\beta}{\hat{h}_{ll}(\omega_0)}\right\} \quad (8)$$

3. Simulations of the control

Different results obtained from the simulation of the control in the time domain for a system composed of 7 coplanar control units at frequency 240 Hz are now presented. The geometrical configuration of the control units used for these simulations is illustrated in figure 3. The physical plant h, was obtained from the experimental values of the 128-order FIR filters that modelled the transfer function between each loudspeaker and each microphone.

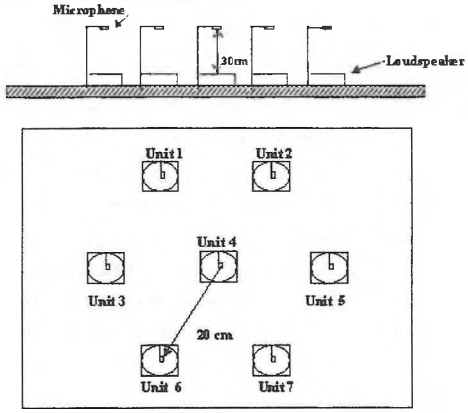

Figure 3: Configuration of the control simulation.

During these simulations, the adaptation process is frozen at different iterations k. The corresponding values of the control filters Γ (modelled by 32-order FIR filter) are then used to calculate the mean values of the performance index β and $L(s,\beta)$.

Figure 4 shows the evolution of the map $L(s,\beta)$ obtained for these different values of the index performance. According to this figure, the stability of the system is affected by the values of β with a decrease of its stability margin when β increases. The control system is find to be stable while the map of $L(s,\beta)$ doesn't encircle the origin which correspond to values of $\beta \leq 0.30$. For β=0.35, the map of $L(s,\beta)$ encircles the origin and the control system is unstable in regard of the Nyquist criterion.

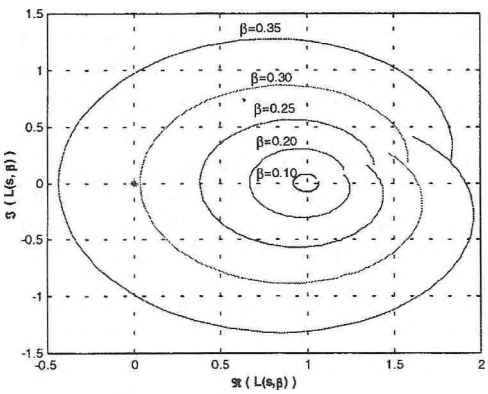

Figure 4: Map of L (s, β) on the Nyquist D-contour obtained for different values of β.

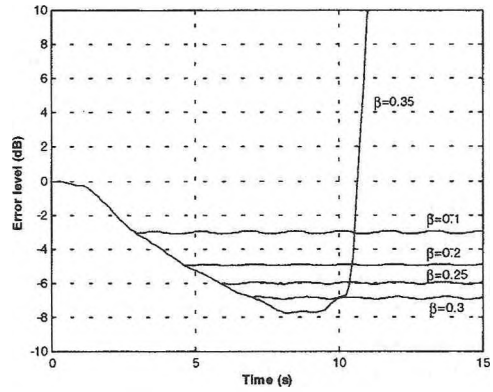

Figure 5: Sum of the temporal squared error signals measured at the microphones for different values of the index performance β.

The sum of the squared error signals at the microphones for the same values of β are represented in figure 5. As observed on this figure, if $\beta \leq 0.30$, the control filters progress on their convergence path while the adaptation process is actuated. The error signal at the microphones decreases for increasing values of β. When the adaptation is frozen, the control filters stop their convergence on a specific value and the error signal at the microphone cease its decrease. For β=0.35, a decrease of the error signal is also noticed at the begining of the adaptation until a large increase of the error signal is observed. This one corresponds to the instability of the control system expected by the Nyquist criterion. This can be explain by the fact that during the adaptation, the control filters reached some values which cause the instability of the feedback loop.

4. Conclusions

This paper presents a decentralized adaptive feedback control system of periodic noise. A condition, derived from the Nyquist criterion, is given in order to predict the stability of the control. It has be shown, that the positions of the control filters on their convergence path play an important role on the stability and the performance of the control system. The control of the parameter β, called performance index wich was associated to these positions, appears thus a good alternative to make a compromise between performance and stability. The manner to control β presented in this paper, was to stop the adaptation of the control filters on the desired values. However, this technique is difficult to implement in practical cases. Others procedures of control of this parameter could be developped and implemented like introducing a leaky coefficient in the LMS algorithm, or reinjecting a proportional part of the estimate signal of the pertubation in the calcul of this same estimate signal of the perturbation realized by the internal model.

References

[1] B. Raphaely, S. J. Elliott, T. J. Sutton and M. Johnson, "Design of feedback controllers using a feedforward approach", Proceeding of Active 95, pp. 863-874, 1995.

[2] E. Leboucher, P. Micheau, A. Berry and A. L'Espérance, "A decentralised adaptive feedback active noise control system of periodic sound in free space", Proceeding of Active 99, pp. 973-984, 1999.